



**Repositorio Institucional de la Universidad Autónoma de Madrid**

<https://repositorio.uam.es>

Esta es la **versión de autor** del artículo publicado en:

This is an **author produced version** of a paper published in:

Angewandte Chemie International Edition 55.1 (2016): 223-227

DOI: <http://dx.doi.org/10.1002/anie.201508854>

**Copyright:** © 2016 Wiley VCH Verlag

El acceso a la versión del editor puede requerir la suscripción del recurso  
Access to the published version may require subscription

# The Role of Multipoint Hydrogen-bond Symmetry on Chelate Cooperativity in Supramolecular Macrocyclizations

Carlos Montoro-García,<sup>[a]</sup> Jorge Camacho-García,<sup>[a]</sup> Ana M. López-Pérez,<sup>[a]</sup> María J. Mayoral,<sup>[a]</sup> Nerea Bilbao,<sup>[a]</sup> and David González-Rodríguez<sup>[a]\*</sup>

**Abstract:** Here, we analyze the intrinsic chelate effect that multipoint H-bonding patterns exert in the overall energy of dinucleoside cyclic systems. Our results indicate that the magnitude of  $EM$  is regulated by the symmetry of the H-bonding pattern, which is reduced by about 3 orders of magnitude when going from the unsymmetric ADD-DAA or DDA-AAD patterns to the symmetric DAD-ADA pattern.

The supramolecular synthesis<sup>[1]</sup> of complex nanostructures with a precision analogous to that found in the natural world requires not only an understanding of the noncovalent interactions involved,<sup>[2]</sup> but also of cooperative and multivalent phenomena that may arise between the individual constituents, since the control of structure and monodispersity depends largely on this issue.<sup>[3]</sup>

A molecule with more than one binding site may assemble into linear (open) or cyclic (closed) structures. Although the size of linear oligomers can be sometimes limited within a certain range, the supramolecular product is commonly a statistical distribution of chain lengths.<sup>[4]</sup> Therefore, the synthesis of discrete supramolecular structures has normally been focused on closed (multi)macrocylic systems, where size and structure are dictated by the geometric requirements of the monomer and the binding interaction.<sup>[5]</sup> The effect that causes the quantitative formation of a particular ring-closed species is defined as *chelate cooperativity*, and stems from the fact that an intramolecular interaction is favored over an intermolecular one, providing a series of conditions of enthalpic and entropic origin are met.<sup>[3]</sup> The increased in stability when comparing a linear and a cyclic oligomer of a certain length is given by the product  $K_{\text{inter}} \cdot EM$ , where  $K_{\text{inter}}$  is the intermolecular binding constant and considers the additional association to form the cycle, whereas  $EM$ , the key parameter quantifying

chelate cooperativity, stands for *effective molarity* and takes into account that this last binding event is intramolecular ( $EM = K_{\text{intra}}/K_{\text{inter}}$ ).<sup>[6]</sup>

In this context, multipoint H-bonding motifs, constituted by an array of vicinal H-bonding donor (D) and acceptor (A) groups, arise as a relevant noncovalent interaction increasingly used to produce not only discrete cyclic assemblies, but also supramolecular polymers and functional materials.<sup>[7]</sup> A relevant example is represented by the nucleobases<sup>[8]</sup> and DNA itself, constituted by combinations of unsymmetric ADD-DAA guanine-cytosine and symmetric DA-AD adenine-thymine H-bonded Watson-Crick pairs, can be regarded as the biological stereotype of a closed assembly. The relative strength of these multipoint H-bonding interactions is now well understood since the work of

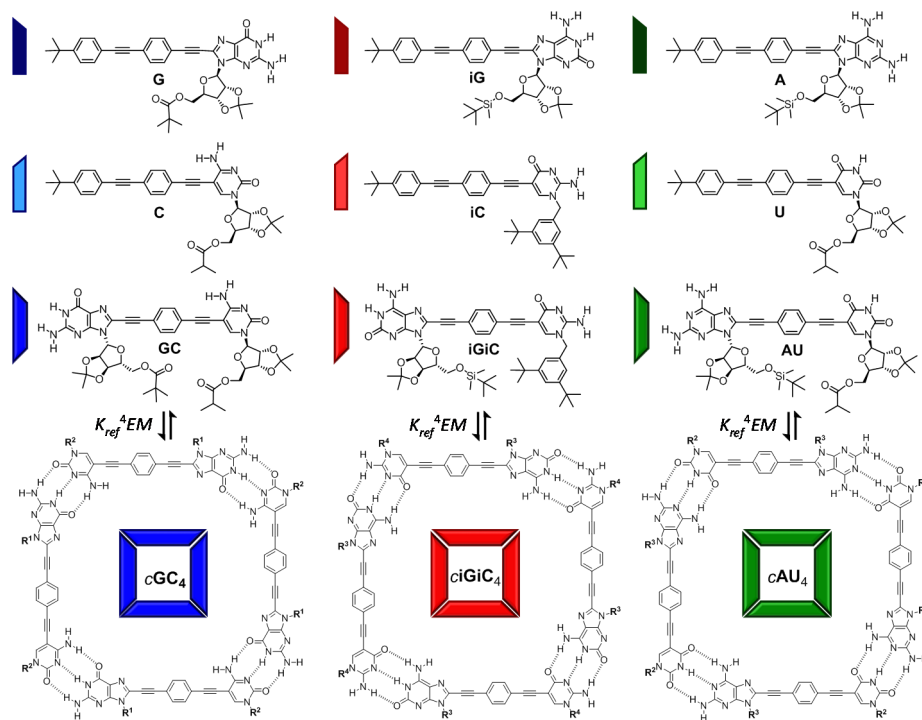


**Figure 1.** Structure of lipophilic dinucleoside monomers **GC**, **iGiC** and **AU** and reference mononucleoside compounds **G**, **C**, **iG**, **iC**, **A** and **U**. Structure of the 3 cyclic tetramers formed in solution **cGC<sub>4</sub>** (ADD-DAA), **ciGiC<sub>4</sub>** (DDA-AAD) and **cAU<sub>4</sub>** (DAD-ADA).

Jorgensen in the 90s.<sup>[9]</sup> His interpretation takes into account secondary electrostatic interactions between contiguous centers to explain the trend in association constants of, for instance, triple H-bonded pairs: DDD-AAA > ADD-DAA > DAD-ADA. However, the intrinsic influence of the H-bonding pattern on  $EM$ , and hence on the chelate cooperativity of a cyclization process, has never been addressed and it is the main focus of this work. For such aim, we compare the self-assembly thermodynamics of 3 related monomers (**GC**, **iGiC**, **AU**) into their respective cyclic tetramers (**cGC<sub>4</sub>**, **ciGiC<sub>4</sub>**, **cAU<sub>4</sub>**; Figure 1). Our results disclose a huge effect

[a] C. Montoro-García, J. Camacho-García, Dr. A. M. López-Pérez, Dr. M. J. Mayoral, N. Bilbao, Dr. D. González-Rodríguez  
Nanostructured Molecular Systems and Materials group  
Departamento de Química Orgánica, Facultad de Ciencias,  
Universidad Autónoma de Madrid, 28049 Madrid, Spain  
E-mail: david.gonzalez.rodriguez@uam.es

Supporting information for this article is given via a link at the end of the document.

of the binding interaction symmetry on the magnitude of  $EM$ , and may be thus highly valuable in the future design of suitable monomers that lead quantitatively to either discrete closed assemblies or, on the other extreme, to supramolecular polymers.

The self-assembly of monomers **GC**, **iGiC** and **AU** was analyzed in different solvents by a wide number of concentration- and temperature-dependent spectroscopic methods (1D and 2D  $^1\text{H}$  NMR, as well as absorption, emission and CD spectroscopy). These experiments were described in our previous work<sup>[10]</sup> and the combined results for the 3 monomers are detailed in the S. I. of this manuscript (Figures S1-S15).<sup>[11]</sup> The equilibrium constants of the cyclotetramerization processes ( $K_T$ ) could be obtained in some of these experiments and are collected in Table 1, together with the reference association constants between complementary mononucleosides ( $K_{ref}$ ). The whole set of results clearly demonstrate that **AU** forms considerably less stable cyclic tetramers than **GC** or **iGiC**, which, on the other hand, reveal comparable qualitative and quantitative association behavior.

**Table 1.** Cyclotetramerization constants ( $K_T$ ), reference intermolecular association constants ( $K_{ref}$ ) and effective molarities ( $EM$ ) obtained for **GC/iGiC/AU** from different experiments.

| <i>M</i>    | <i>Solvent</i>                       | $K_T$<br>$\text{M}^{-3}$                  | $K_{ref}^a$<br>$\text{M}^{-1}$ | $EM$<br>$\text{M}$  |
|-------------|--------------------------------------|---|--------------------------------|---------------------|
| <b>GC</b>   | DMF                                  | $2.3 \pm 0.8 \times 10^5$ <sup>b</sup>    | $5.7 \pm 0.3$                  | 218                 |
|             | THF                                  | $9.1 \pm 4.0 \times 10^{14}$ <sup>c</sup> | $1.5 \pm 0.1 \times 10^3$      | 180                 |
|             |                                      | $3.7 \pm 0.3 \times 10^{15}$ <sup>d</sup> |                                | 730                 |
|             | $\text{CHCl}_3$                      | $5.6 \pm 3.1 \times 10^{20}$ <sup>e</sup> | $2.8 \pm 0.3 \times 10^4$      | 910                 |
|             |                                      | $5.0 \pm 0.1 \times 10^{20}$ <sup>f</sup> |                                | 813                 |
| <b>iGiC</b> | DMF                                  | $3.4 \pm 1.9 \times 10^5$ <sup>b</sup>    | $6.1 \pm 0.8$                  | 246                 |
|             | THF                                  | $3.7 \pm 1.2 \times 10^{15}$ <sup>c</sup> | $1.7 \pm 0.6 \times 10^3$      | 463                 |
|             |                                      | $2.2 \pm 0.5 \times 10^{15}$ <sup>d</sup> |                                | 294                 |
|             | $\text{CHCl}_3$                      | $3.3 \pm 0.4 \times 10^{20}$ <sup>f</sup> | $3.2 \pm 0.5 \times 10^4$      | 314                 |
| <b>AU</b>   | $\text{CHCl}_3$                      |   | $2.5 \pm 0.4 \times 10^2$      | $0.10$ <sup>h</sup> |
|             | $\text{CHCl}_3/\text{CCl}_4$ (2:3)   | $9.4 \pm 0.3 \times 10^{11}$ <sup>c</sup> | $2.0 \pm 0.4 \times 10^3$      | 0.06                |
|             |                                      | $2.8 \pm 0.2 \times 10^{11}$ <sup>d</sup> |                                | 0.02                |
|             | $\text{CHCl}_3/\text{Acetone}$ (5:1) | $7.2 \pm 1.6 \times 10^9$ <sup>g</sup>    | $0.9 \pm 0.6 \times 10^2$      | 0.11                |

<sup>a</sup> Determined from titration experiments with the mononucleosides: **G+C**, **iG+iC**, **A+U**.<sup>[12]</sup> Data calculated from: <sup>b</sup>  $^1\text{H}$  NMR dilution (Figure S9). <sup>c</sup> UV-vis dilution (Figure S13). <sup>d</sup> Temperature-dependent experiments (Figure S14). <sup>e</sup>  $^1\text{H}$  NMR competition (Figure S15). <sup>f</sup> Fluorescence competition (Figure S16). <sup>g</sup>  $^1\text{H}$  NMR dilution (Figure S7B). <sup>h</sup> Estimated from the fitting of the  $^1\text{H}$  NMR dilution data (see Figures S1 and 2c).

This stability trend was expected, since the individual **A:U** binding constant ( $K_{ref} \sim 2.5 \times 10^2 \text{ M}^{-1}$ ) is typically about 2 orders of magnitude lower than **G:C** or **iG:iC** ( $K_{ref} \sim 3 \times 10^4 \text{ M}^{-1}$ ) in  $\text{CHCl}_3$ .<sup>[12]</sup> This can be explained by the different stabilizing/destabilizing secondary H-bonding interactions between vicinal donor and acceptor groups in the DAD-ADA (**A:U**) pair *versus* the DDA-ADD (**G:C** or **iG:iC**) pair.<sup>[9]</sup> However, the experimental results obtained in this work and exposed in Table 1, suggest that such reduction is actually much larger. In fact, as explained below, our results indicate that  $K_T$  for **AU** is not only reduced by a decrease in  $K_{ref}$ , but also by a substantial decrease in the magnitude of  $EM$ .

In order to evaluate this hypothesis, competition experiments were performed in which increasing amounts of the corresponding complementary pyrimidine mononucleoside (**C/iC/U**) are gradually added to a solution of the associated tetramers (**cGC<sub>4</sub>/ciGiC<sub>4</sub>/cAU<sub>4</sub>**) (Figure S15 and S16). The titration process was monitored in solvents of low polarity by two different techniques:  $^1\text{H}$  NMR at high concentrations (*ca.*  $10^{-2}$  M) and emission spectroscopy at relatively low concentrations (*ca.*  $10^{-4}$  M). Our results, summarized in Figure 2a, show that while **cGC<sub>4</sub>/ciGiC<sub>4</sub>** can resist up to 60 equivalents of **C/iC** mononucleosides, **cAU<sub>4</sub>** was fully dissociated after the addition of *ca.* 3 **U** equivalents, independently of the solvent system employed, indicating a much weaker chelate effect in **cAU<sub>4</sub>**. These experiments, where the intramolecular and intermolecular base pair binding events are made to compete, constitute the most appropriate way to detach the intrinsic contribution of the chelate cooperativity from the overall energy of the system. As a matter of fact, the  $EM$  of the system can be inversely related to the competition equilibrium constant ( $K_C$ ) as:  $EM = 1/K_C$ .<sup>[11]</sup>

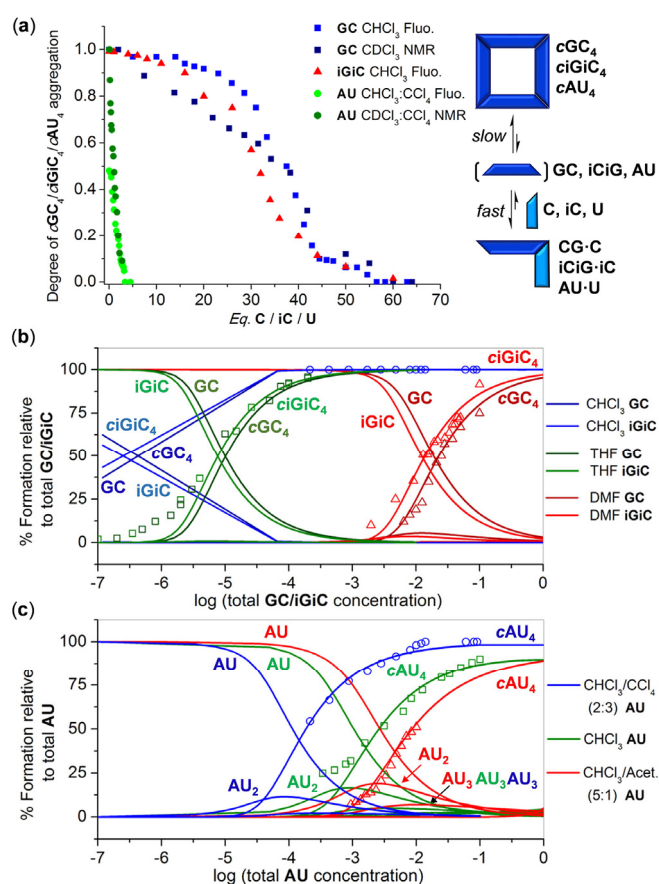


**Figure 2.** (a) Competition experiments. Plots of the degree of **cGC<sub>4</sub>**, **ciGiC<sub>4</sub>** and **cAU<sub>4</sub>** association, measured by either  $^1\text{H}$  NMR or fluorescence spectroscopy, as a function of the equivalents of **C/iC/U** added. (b, c) Simulated speciation curves (lines) and experimental dilution data (circles/triangles/squares) indicating the degree of **cM<sub>4</sub>** association of (b) **GC/iGiC** in  $\text{CHCl}_3$  (Figure S1), THF (Figure S13A,B) and DMF (Figure S9), and (c) **AU** in  $\text{CHCl}_3/\text{CCl}_4$  (2:3) (Figure S13C),  $\text{CHCl}_3$  (Figure S1) and  $\text{CHCl}_3/\text{Acetone}$  (5:1) (Figure S7B).

The  $EM$  values for each cyclotetramerization process (Table 1) were calculated from the  $K_T$  values and the corresponding  $K_{ref}$

constants obtained in the different experiments,<sup>[10,12]</sup> using the relationship:  $EM = K_T / K_{ref}^4$ . These  $K_{ref}$  and  $EM$  values were also used to simulate speciation curves for each dinucleoside in different solvent systems (Figure 2b,c). These curves, which relate the concentration of each supramolecular species with total concentration, are able to reproduce quite satisfactorily the dissociation trends observed for **cGC**<sub>4</sub>/**ciGiC**<sub>4</sub>/**cAU**<sub>4</sub> in dilution experiments.<sup>[11]</sup> In all cases, **cGC**<sub>4</sub> and **ciGiC**<sub>4</sub> fulfill the condition  $K_{ref} \cdot EM > 185 \cdot n$ , ( $n$  being the number of monomers in the cycle;  $n = 4$ ), defined by Ercolani to reach complete cycle assembly.<sup>[6]</sup> However, the concentration range where this condition is met is clearly wider in solvents that do not compete strongly for H-bonding and thus maintain a high  $K_{ref}$  value. On the contrary,  $EM$  values between 0.05 and 0.1 had to be set to reproduce appropriately the dilution trends of **cAU**<sub>4</sub> in three solvent systems. This represents a reduction of more than 3 orders of magnitude in  $EM$  with respect to the **GC/iGiC** cyclization process. As a result, and in line with our experimental observations, the condition  $K_{ref} \cdot EM > 185 \cdot n$  is hardly fulfilled by **AU** even in the highly apolar **CHCl**<sub>3</sub>/**CCl**<sub>4</sub> (2:3) mixture, where  $K_{ref}$  is enhanced.

All monomers share a common, rigid structure that was designed to produce cyclic squared-shaped assemblies devoid of strain and with minimal conformational entropy loss. This was achieved, on one hand, profiting from the 90° angle that the 8-purine and 5-pyrimidine positions adopt upon Watson-Crick complementary base pairing, and, on the other, employing a rigid central block connecting the bases with only 4 rotatable linear  $\pi$ -conjugated bonds. As shown in Figure 3a, rotation around these bonds can produce different conformations in which the Watson-Crick edges alternate between *syn* and *anti* relative arrangements. However, cycle formation demands the Watson-Crick edges to be in a *syn* relative conformation. This is a degree of freedom that is lost when comparing cyclic and open **GC**, **iGiC**, and **AU** oligomers, and must contribute to a reduction, of entropic origin, in the maximum attainable  $EM$  of the cyclic system. Now, the **AU** monomer, having complementary nucleosides that pair with a symmetric DAD-ADA H-bonding pattern, have the possibility to self-assemble *via* either Watson-Crick or reverse Watson-Crick interactions (Figure 3a). Each binding mode provides a different association angle (90° and 210°) and their relative energy is assumed to be comparable, as previous studies with the adenine-thymine pair have demonstrated.<sup>[13,14]</sup> This introduces additional degrees of freedom, not available in the unsymmetric ADD-DAA or DDA-AAD patterns, that allow the linear **AU** <sub>$n$</sub>  oligomers to access a higher number of binding and conformational possibilities. However, such freedom must be lost upon cycle formation because the cyclotetramerization process exclusively demands a 90° Watson-Crick interaction. Hence, we assume that the entropy loss associated to cyclization becomes much larger for **cAU**<sub>4</sub> than for **cGC**<sub>4</sub> or **ciGiC**<sub>4</sub>, resulting in a supplementary and notable reduction of the  $EM$  values.<sup>[15]</sup>

It would have been highly interesting to compare the cyclization process of our **AU**, **GC** and **iGiC** molecules with a related dinucleoside having complementary DDD-AAA base pairs. However, a purine-pyrimidine couple having such H-bonding pattern and that would maintain the same geometric requirements is simply not available. We propose, given the conclusions drawn from this work, that such cyclic tetramer bound

by symmetric DDD-AAA pairs would be endowed with both a high  $K_{ref}$  (ca.  $10^5$ – $10^6$  M in **CHCl**<sub>3</sub>, as reported in the literature)<sup>[7a]</sup> and a low  $EM$  (0.01–0.1, comparable to **cAU**<sub>4</sub>), due to the possibility of binding with two different angles. From these values, we simulated in Figure 3b the speciation curves of this hypothetical symmetric DDD-AAA system in **CHCl**<sub>3</sub> and compared it with the ones obtained for unsymmetric ADD-DAA/DDA-AAD and symmetric DAD-ADA H-bonded systems.

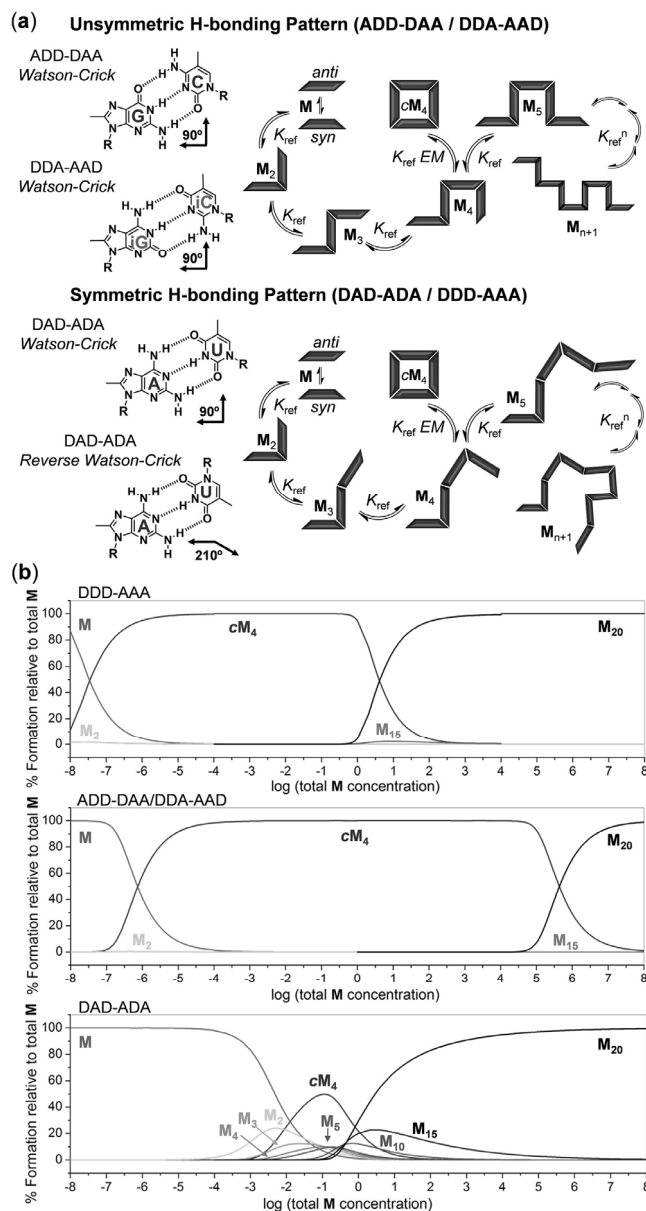


**Figure 3.** (a) Unsymmetric *versus* Symmetric H-bonding patterns. (b) Simulated speciation curves for the H-bonded self-assembly of a hypothetical DDD-AAA ( $K_{ref} = 10^6$  M<sup>-1</sup>;  $EM = 0.05$  M), ADD-DAA/DDA-AAD ( $K_{ref} = 10^4$  M<sup>-1</sup>;  $EM = 500$  M), and DAD-ADA ( $K_{ref} = 10^2$  M<sup>-1</sup>;  $EM = 0.05$  M) ditopic monomers with identical geometrical features to the ones studied in this work. For the sake of clarity, only a few supramolecular species are represented within the  $10^{-8}$  to  $10^8$  M concentration range: **M**, **M**<sub>2</sub>, **M**<sub>3</sub>, **M**<sub>4</sub>, **cM**<sub>4</sub>, **M**<sub>5</sub>, and, as examples of higher-order H-bonded linear oligomers: **M**<sub>10</sub>, **M**<sub>15</sub>, and **M**<sub>20</sub>.

It is clear that the use of a ADD-DAA/DDA-AAD H-bonding pattern, providing moderate  $K_{\text{ref}}$  and high  $EMs$ , leads to cyclic tetramer assemblies that persist as the main species in solution over a much broader concentration range. Only at very low concentrations  $cM_4$  is dissociated as a monomer, but no other associated species is seen to compete within the  $10^{-8}$  to  $10^5$  M concentration range, underlining the strong all-or-nothing behavior of this H-bonded system. At very high concentrations intra- and intermolecular processes begin to compete, and above  $10^5$  M linear polymers of high molecular weight grow at the expense of the  $cM_4$  species. On the other hand, the DDD-AAA pattern leads to more strongly bound assemblies along the whole concentration scale, as a result of a high  $K_{\text{ref}}$  value, and the monomer is only present at concentrations below  $10^{-5}$  M. The  $cM_4$  species is dominant between the  $10^{-5}$ –1 M range but, in sharp contrast to the unsymmetric pattern, higher-order linear oligomers begin to compete strongly at moderate concentrations. Finally, in the weaker DAD-ADA H-bonded system no associated species is seen below  $10^{-4}$  M. At intermediate concentrations a distribution of small oligomers, among which  $cM_4$  is one of the main species, is observed. In analogy to the DDD-AAA system, increasing concentration above 1 M makes the higher-order linear oligomers to dominate. However, high molecular weight distributions are much faster attained with the DDD-AAA system than with the DAD-ADA H-bonding pattern, as a result of a  $K_{\text{ref}}$  that is about 4 orders of magnitude higher. It should be noted that the quantitative results derived from Figure 3b must be strictly applied to the specific monomer geometries studied in this work.

In summary, in this work we have been able to dissect and analyze independently the contributions of the H-bonding strength between complementary nucleobases, explained by the Jorgensen model, and the intrinsic chelate effect that they exert in cyclic systems. The results presented clearly demonstrate that cyclic assemblies constructed from symmetric DAD-ADA H-bonding pairs are much less stable than the homologues associated from unsymmetric ADD-DAA or DDA-AAD pairs. On one hand, the DAD-ADA bonding pattern reduces considerably the enthalpy of intermolecular association due to the absence of attractive secondary interactions between vicinal H-bonding groups. On the other, the symmetry of this pattern introduces the possibility of multiple binding modes and hence a higher number of degrees of freedom in linear oligomers, which are then lost upon macrocyclization. This effect, of entropic origin, has a large impact on the  $EM$  of the system, which in our case is reduced by about 3 orders of magnitude. Our conclusions could in principle be extended to many linear or cyclic supramolecular systems assembled *via* multipoint binding interactions. If a discrete, well-defined closed architecture is to be designed, rigid monomers with a suitable geometry in combination with an unsymmetric binding motif should be used to enhance the  $EMs$  of the cyclization process. In other words, the binding interaction should also contribute to the preorganization of the system towards a specific structure, reducing the degrees of freedom of any other competitive supramolecular species. If, on the other hand, linear supramolecular polymers are pursued, a strong symmetric multipoint binding interaction would be the best choice to minimize chelate cooperativity, and hence the tendency of the supramolecular system to form undesired cycles.

## Acknowledgements

Funding from the European Union (*ERC-Starting Grant 279548*) and MINECO (*CTQ2011-23659* and *CTQ2014-57729-P*) is gratefully acknowledged.

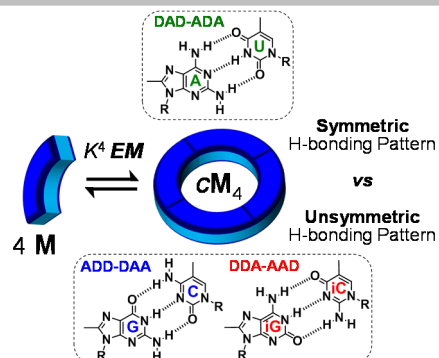
**Keywords:** Supramolecular Chemistry • Noncovalent Synthesis • Chelate Effect • Nucleoside Self-assembly • Effective Molarity

- [1] a) L. J. Prins, D. N. Reinhoudt, P. Timmerman, *Angew. Chem. Int. Ed.* **2001**, *40*, 2382–2426; *Angew. Chem.* 2001, *113*, 2446–2492; b) D. N. Reinhoudt, M. Crego-Calama, *Science* **2002**, *295*, 2403–2407.
- [2] D. González-Rodríguez, A. P. H. J. Schenning, *Chem. Mater.* **2011**, *23*, 310–325.
- [3] a) J. D. Badjić, A. Nelson, S. J. Cantrill, W. B. Turnbull, J. F. Stoddart, *Acc. Chem. Res.* **2005**, *38*, 723–732; b) Focus Issue on Cooperativity. *Nat. Chem. Biol.* **2008**, *4*, 433–507; c) C. A. Hunter, H. L. Anderson, *Angew. Chem. Int. Ed.* **2009**, *48*, 7488–7499; *Angew. Chem.* **2009**, *121*, 7624–7636; d) G. Ercolani, L. Schiaffino, *Angew. Chem. Int. Ed.* **2011**, *50*, 1762–1768; *Angew. Chem.* **2011**, *123*, 1800–1807.
- [4] T. F. A. de Greef, M. M. J. Smulders, M. Wolffs, A. P. H. J. Schenning, R. P. Sijbesma, E. W. Meijer, *Chem. Rev.* **2009**, *109*, 5687–5754.
- [5] a) M. Fujita, M. Tominaga, A. Hori, B. Therrien, *Acc. Chem. Res.* **2005**, *38*, 371–380; b) M. J. Mayoral, N. Bilbao, D. González-Rodríguez, *ChemistryOpen*, **2015**, DOI: 10.1002/open.201500171.
- [6] a) G. Ercolani, *J. Phys. Chem. B*, **1998**, *102*, 5699–5703; b) G. Ercolani, *J. Phys. Chem. B*, **2003**, *107*, 5052–5057; c) G. Ercolani, *Struct. Bond.* **2006**, *121*, 167–215; d) H. Sun, C. A. Hunter, C. Navarro, S. Turega, *J. Am. Chem. Soc.* **2013**, *135*, 13129–13141.
- [7] a) T. F. A. de Greef, E. W. Meijer, *Nature*, **2008**, *453*, 171–173; b) B. A. Blight, C. A. Hunter, D. A. Leigh, H. McNab, P. I. T. Thomson, *Nature Chem.* **2011**, *3*, 244–248; c) S. K. Yang, S. C. Zimmerman, *Isr. J. Chem.* **2013**, *53*, 511–520.
- [8] a) S. Sivakova, S. J. Rowan, *Chem. Soc. Rev.* **2005**, *34*, 9–21; b) J. L. Sessler, C. M. Lawrence, J. Jayawickramarajah, *Chem. Soc. Rev.* **2007**, *36*, 314–325; c) M. Fathalla, C. M. Lawrence, N. Zhang, J. L. Sessler, J. Jayawickramarajah, *Chem. Soc. Rev.* **2009**, *38*, 1608–1620.
- [9] W. L. Jorgensen, J. Pranata, *J. Am. Chem. Soc.* **1990**, *112*, 2008–2010.
- [10] a) C. Montoro-García, J. Camacho-García, A. M. López-Pérez, N. Bilbao, S. Romero-Pérez, M. J. Mayoral, D. González-Rodríguez, *Angew. Chem. Int. Ed.* **2015**, *54*, 6780–6784; *Angew. Chem.* **2015**, *127*, 6884–6888; b) S. Romero-Pérez, J. Camacho-García, C. Montoro-García, A. M. López-Pérez, A. Sanz, M. J. Mayoral, D. González-Rodríguez, *Org. Lett.* **2015**, *17*, 2664–2667.
- [11] See the Supporting information for further details.
- [12] J. Camacho-García, C. Montoro-García, A. M. López-Pérez, N. Bilbao, S. Romero-Pérez, D. González-Rodríguez, *Org. Biomol. Chem.* **2015**, *13*, 4506–4513.
- [13] a) R. L. Ornstein, J. R. Fresco, *Proc. Natl. Acad. Sci. U. S. A.* **1983**, *80*, 5171–5175; b) S. N. Rao, P. A. Kollman, *Biopolymers*, **1986**, *25*, 267–280.
- [14] Additional A-U binding modes could be considered that do not differ much in association strength from the Watson-Crick mode, such as the double H-bonding interaction of the U base with the 2-aminoadenine Hoogsten edge.
- [15] It is interesting to note that related cyclic tetramers based on pyridine-metal coordination, a strong, single-point interaction that allows for some degree of torsional and rotational flexibility, afford  $EM$  values that are intermediate between our symmetric and unsymmetric patterns ( $EM = 0.1$ – $20$  M). We would also like to remark, as previous studies have also shown (see ref 6d), that these supramolecular  $EMs$  do not seem to follow any clear relationship with solvent polarity or H-bond strength.

## Entry for the Table of Contents

### COMMUNICATION

The **symmetry** of the hydrogen-bonding pattern is demonstrated to greatly influence the chelate effect in a supramolecular cyclization process.



*Carlos Montoro-García, Jorge Camacho-García, Ana M. López-Pérez, María J. Mayoral, Nerea Bilbao and David González-Rodríguez\**

**Page No. – Page No.**

**The Role of Multipoint Hydrogen-bond Symmetry on Chelate Cooperativity in Supramolecular Macrocyclizations**